Am J Physiol Cell Physiol 292: C1809–C1815, 2007.
First published 31 January 2006; doi:10.1152/ajpcell.00580.2006.

Apoptosis-associated tyrosine kinase scaffolding of protein phosphatase 1 and SPAK reveals a novel pathway for Na-K-2C1 cotransporter regulation

Kenneth B. E. Gagnon, Roger England, Lisa Diehl, and Eric Delpire

Department of Anesthesiology, Vanderbilt University Medical Center, Nashville, Tennessee

Submitted 17 November 2006; accepted in final form 24 January 2007

Gagnon KB, England R, Diehl L, Delpire E. Apoptosis-associated tyrosine kinase scaffolding of protein phosphatase 1 and SPAK reveals a novel pathway for Na-K-2C1 cotransporter regulation. *Am J Physiol Cell Physiol* 292: C1809–C1815, 2007. First published 31 January 2006; doi:10.1152/ajpcell.00580.2006.—Previous work from our laboratory and others has established that Ste-20-related proline-alanine-rich kinase (SPAK/PASK) is central to the regulation of NKCC1 function. With no lysine (K) kinase (WNK4) has also been implicated in the regulation of NKCC1 activity through upstream activation of SPAK. Because previous studies from our laboratory also demonstrated a protein-protein interaction between SPAK and apoptosis-associated tyrosine kinase (AATYK), we explore here the possibility that AATYK is another component of the regulation of NKCC1. Heterologous expression of AATYK1 in NKCC1-injected *Xenopus laevis* oocytes markedly inhibited cotransporter activity under isosmotic conditions. Interestingly, mutation of key residues in the catalytic domain of AATYK1 revealed that the kinase activity does not play a role in the suppression of NKCC1 function. However, mutagenesis of the two SPAK-binding motifs in AATYK1 completely abrogated this effect. As protein phosphatase 1 (PP1) also plays a central role in the dephosphorylation and inactivation of NKCC1, we investigated the possibility that AATYK1 interacts with the phosphatase. We identified a PP1 docking motif in AATYK1 and demonstrated interaction using yeast-2-hybrid analysis. Mutation of a key valine residue (V1175) within this motif prevented protein-protein interaction. Furthermore, the physical interaction between PP1 and AATYK was required for inhibition of NKCC1 activity in *Xenopus laevis* oocytes. Taken together, our data are consistent with AATYK1 indirectly inhibiting the SPAK/WNK4 activation of the cotransporter by scaffolding an inhibitory phosphatase in proximity to a stimulatory kinase.

ion fluxes; *Xenopus laevis* oocytes; yeast-2 hybrid; phosphorylation

PROTEIN KINASES and protein phosphatases exert coordinated control over many essential cellular processes by catalyzing opposing reversible phosphorylation reactions (37). The Na-K-2Cl cotransporter (NKCC1) is a membrane transport protein involved in cell volume regulation, cell proliferation and survival, epithelial transport, neuronal excitability, and blood pressure control (for review, see Ref. 33). Several studies suggest that the regulation of NKCC1 activity by phosphorylation/dephosphorylation mechanisms involves multiple kinases and phosphatases (22). Recent work from our laboratory (29, 30) has identified an association between the widely expressed NKCC1 and two Ste20p-like serine/threonine kinases, Ste20p-related proline alanine-rich kinase (SPAK) and oxidative stress response 1 (OSR1). SPAK/OSR1 mediates phosphorylation of NKCC1 leading to its activation. Importantly, Ste20p-likep kinases are themselves under the control of upstream kinases, such as with no lysine (K) kinases, WNK1 and WNK4, suggesting a cascade of phosphorylation events involving multiple kinases (15, 26, 35).

In 1997, Gaozza and coworkers identified a novel gene whose expression was dramatically upregulated during growth arrest and apoptosis of myeloid cells. This gene encodes for a putative tyrosine kinase that the authors termed apoptosis-associated tyrosine kinase (AATYK) (16). Murine AATYK1 consists of 1,317 amino acids with an amino terminal putative kinase domain and a long carboxyl-terminal "regulatory" domain. Recently, a review of human tyrosine kinases identified the location of genes encoding three separate AATYKs: AATYK1 on human chromosome 17, AATYK2 (or BREK/KPI-1/CPRK) on chromosome 7, and AATYK3 on chromosome 19 (32). Their sequence analysis reveals a conserved serine residue NH_2-terminal to the DLALRN motif, suggesting the possibility that AATYKs are multispecific kinases (functioning as both a Y and S/T kinase). AATYKs possess several potential SH3 domain binding sites (PxxP-motifs) in the COOH-terminal region, indicating multiple potential sites of protein interaction. Unlike the cytosolic AATYK1, AATYK2 and AATYK3 contain two conserved hydrophobic sequences in their NH_2-terminus that may facilitate membrane localization (19).

AATYK1 is a nonreceptor type tyrosine kinase, which is predominantly expressed in adult brain, but also found at lower levels in tissues such as kidney, heart, lung, liver, and skeletal muscle (16, 34). Along with apoptotic function, AATYK1 has also been shown to promote neuronal differentiation (3, 19, 31). We recently demonstrated protein-protein interaction between AATYK1 and SPAK and identified two putative (R/KFxV/I) binding motifs within the regulatory domain of AATYK1 (29). The presence of these SPAK binding motifs, along with the SH3 binding motifs suggests that AATYK1 likely interacts with a variety of proteins that modulate intracellular signaling (4).

In this study, we demonstrate that heterologous expression of AATYK1 and NKCC1 in *Xenopus laevis* oocytes results in a significant reduction in cotransporter activity. Because of the putative interaction between AATYK1 and SPAK, which likely occurs at one or both of the regulatory domain binding motifs, we postulate that AATYK1 modulates NKCC1 function through its interaction with the Ste20 kinase.

EXPERIMENTAL PROCEDURES

Cloning of mouse protein phosphatase 1. The open reading frame of mouse protein phosphatase 1 (PP1) was amplified from cDNA reverse transcribed from mouse brain using sense and antisense

Address for reprint requests and other correspondence: E. Delpire, Dept. Anesthesiology, T-4202 MCN, 1161 21st Ave. S., Nasvhille, TN 37232-2520 (e-mail: eric.delpire@vanderbilt.edu).

The costs of publication of this article were defrayed in part by the payment of page charges. The article must therefore be hereby marked "*advertisement*" in accordance with 18 U.S.C. Section 1734 solely to indicate this fact.

 0363-6143/07 $8.00 Copyright © 2007 the American Physiological Society

Downloaded from http://ajpcell.physiology.org/ by 10.220.33.1 on April 19, 2017

oligonucleotide primers. Adaptors made of complimentary oligonucleotides (*Spe*I-*Eco*RI at the 5′ end and *Xho*I-*Kpn*I at the 3′ end) were used to move the full-length mouse PP1 into the yeast pACT2 and pGBDUc2 vectors. Full-length PP1 was also subcloned into the mammalian expression vector pCDNA3 containing a 5′ hemagglutinin (HA) epitope.

Cloning of mouse AATYK1. Sense and antisense oligonucleotide primers were designed to amplify, by PCR, the open reading frame of mouse AATYK1 in two pieces ~2,000 bp each. High-fidelity, long-range PCR was performed using cDNA reverse transcribed from mouse brain, Expand Long Template PCR buffer, and DNA polymerase mix (Roche Applied Science, Indianapolis, IN). After separation of the PCR reactions using 1% agarose gel electrophoresis, we gel extracted (Qiagen, Valencia, CA) the two ~2,000-bp bands and ligated each of them into the TA cloning vector pGEM-Teasy (Invitrogen, Carlsbad, CA). Several clones were isolated to verify proper sequence, and a full-length AATYK1 clone free of mutations was assembled from two of these clones and inserted into the *Xenopus laevis* pBF expression vector using *Eco*RI-*Not*I restriction sites.

Mutagensis of mouse AATYK1. We subcloned a 151 bp NarI-NcoI fragment of the mouse AATYK1 cDNA into a pBSK vector containing a modified multiple cloning site. Then, we mutated the two putative SPAK-binding motifs (RFTV and RFSI) using forward and reverse PCR primers that altered the phenylalanine-1280 residue and phenylalanine-1290 residue into alanines, respectively (QuickChange; Stratagene, La Jolla, CA). The parental DNA was digested with *Dpn*I to cleave methylated GATC sequences. After *Dpn*I treatment of the PCR reaction, a 1-μl aliquot was transformed into *Escherichia coli.* Several clones were isolated to verify proper sequence and mutation. The *NarI-NotI* fragment was then reinserted into the original AATYK1 clone, creating AATYK1 (F1280A;F1290A) in pBF and pACT2 vectors. We also mutated conserved residues that are key to the catalytic activity of AATYK. Complementary sense and antisense oligonucleotides containing the codon GAG (Glu) instead of AAG (Lys) were used to mutate a 400-bp *Eco*RI-*Apa*I fragment from mouse AATYK1 subcloned into pBSK. Similarly, two aspartic acid residues (D206, D224) were also mutated into alanine residues in a 654-bp *Nco*I-*Sac*II fragment from mouse AATYK1. The mutated *Eco*RI-*Apa*I and *Nco*I-*Sac*II fragments were then reinserted into the original clone in pBF. Finally, we mutated a key valine residue in the PP1 docking motif of AATYK1. Complementary sense and antisense oligonucleotides containing the codon GCG (Ala) instead of GTG (Val) were used to mutate a 655-bp *Eag*I-*Eag*I fragment from mouse AATYK1 subcloned into pBSK. After confirmatory sequencing, the mutated *Eag*I-*Eag*I fragment was then reinserted into the original clone in pBF and pGBDUc2 vectors. With the use of forward and reverse PCR primers, a 436-bp fragment was generated to introduce the c-myc epitope at the NH_2-terminus of AATYK1. With the use of *Eco*RI and *Apa*I, the PCR fragment was then substituted into the original AATYK1 clone in pCDNA3. COOH-terminal fragments containing the SPAK and PP1 binding motif mutations were then subcloned into the wild-type c-myc-tagged AATYK1 construct using *Sac*II and *Not*I restriction enzymes.

Yeast two-hybrid. Full-length PP1 and portions of PCR-amplified NKCC1 or AATYK1 were inserted in the Gal4 binding domain yeast vector (pGBDUc2) and transformed into competent PJ69-4A yeast. Competent yeast colonies containing PP1, NKCC1, or AATYK1 in pGBDUc2 were selected from single dropout (−uracil) plates. These were then transformed with either the regulatory domain of SPAK, full-length WNK4, full-length PP1, or regulatory domain of AATYK1 inserted in the GAL4 activating domain yeast vector (pACT2). The transformed yeast were plated on double-dropout (−uracil, −leucine) plates as a control for measuring transformation efficiency and triple dropout (−uracil, −leucine, −histidine) plates to select for protein-protein interaction. Yeast survival was assessed after 2–4 days at 30°C.

Immunoprecipitation and Western blot analysis. Human embryonic kidney (HEK293-FT) cells were transfected with HA-tagged PP1, wild-type SPAK, and one of three c-myc-tagged AATYK1s (wt, F1280A + F1290A, and V1175A) in pCDNA3 at a ratio of 1 DNA: 3 fugene 6 (Roche). Transfected cells were incubated at 37°C/5% CO_2 for 48 h, then lysed with a buffer containing 150 mM NaCl, 50 mM Tris-Cl, 2 mM EDTA, and 1% (vol/vol) Nonidet P-40. Cell lysates were incubated with either monoclonal anti-c-myc, anti-HA, or polyclonal anti-SPAK antibodies overnight at 4°C. Protein A sepharose beads were then added and incubated for an additional 2 h at 4°C. After several washes in lysis buffer, the beads were resuspended in Laemmli sample buffer and denatured at 70°C for 15 min. Immunoprecipitations were then resolved by 9% SDS-PAGE and electroblotted onto polyvinylidene difluoride (PVDF) membranes. Membranes were blocked for 2 h at room temperature with 5% nonfat dry milk in TBST (150 mM NaCl, 10 mM Tris·HCl, 0.5% Tween 20). Membranes were then subjected to either anti c-myc, anti-HA, or anti-SPAK antibodies (1:1,000) in TBST/5% nonfat dry milk overnight at 4°C, washed extensively in TBST, and incubated for 1 h with horseradish peroxidase-conjugated secondary antibodies (1:5,000) in TBST/5% nonfat dry milk. After extensive washing, protein bands were visualized by enhanced chemiluminescence (ECL plus, Amersham Biosciences, Piscataway, NJ).

cRNA synthesis. All cDNA clones in pBF were linearized with *Mlu*I and transcribed into cRNA using a transcription system (mMESSAGE mMACHINE SP6; Ambion, Austin, TX). RNA quality was verified by gel electrophoresis (1% agarose/0.693% formaldehyde), and RNA was quantitated by measurement of absorbance at 260 nm.

Isolation of Xenopus laevis oocytes. Stages V and VI *Xenopus laevis* oocytes were isolated from 8 different frogs as previously described (15, 29) and maintained at 16°C in modified L15 medium (Leibovitz's L15 solution diluted with water to a final osmolarity of 195–200 mOsM and supplemented with 10 mM HEPES and 44 μg gentamicin sulfate). Oocytes were injected on *day 2* with 50 nl water containing 15 ng of NKCC1 cRNA and on *day 3* with 50 nl of water containing 10 ng of each kinase cRNA. Control oocytes were injected with 50 nl of water. ^{86}Rb uptakes were performed on *day 5* postisolation.

Assessment of mouse NKCC1 expression in oocyte plasma membranes. The surface expression of NKCC1 in the oocyte plasma membrane was measured by fluorescence using an EGFP-NKCC1 construct (15). Individual oocytes were monitored for EGFP fluorescence using a Zeiss confocal laser-scanning microscope LSM510 (Plan-Apochromat ×5 objective, 0.16 numerical aperture lens). Excitation wavelength was set at 488 nm, and emission signals were collected using a 505 nm band-pass filter. Gain and offset were manually adjusted to contain the EGFP fluorescence signal within the 0–215 intensity range of the 8-bit gray density scale. We captured a Z-stack of six optical slices near the middle of the oocyte and chose a single optical section with the largest diameter, indicative of the equatorial center of the oocyte. These settings were used to assess fluorescence of EGFP-NKCC1 in the presence and absence of AATYK1.

K^+ uptakes in Xenopus laevis oocytes. Groups of 20 oocytes in a 35-mm dish were washed once with 3 ml of isosmotic saline composed of (in mM) 96 NaCl, 4 KCl, 2 $CaCl_2$, 1 $MgCl_2$, and 5 HEPES buffered to pH 7.4, and preincubated for 15 min in 1 ml of the same isosmotic saline containing 1 mM ouabain. The solution was then aspirated and replaced with 1 ml isosmotic flux solution containing 5 μCi ^{86}Rb. Two 5-μl aliquots of flux solution were sampled at the beginning of each ^{86}Rb uptake period and used to determine specific activity. After 1-h uptake, the radioactive solution was aspirated and the oocytes were washed 4 times with 3 ml ice-cold isosmotic solution. Single oocytes were transferred into glass vials, lysed for 1 h with 200 μl 0.25N NaOH, neutralized with 100 μl glacial acetic acid, and ^{86}Rb tracer activity was measured by β-scintillation counting. NKCC1 flux is expressed in nanomoles K^+/oocyte/h.

Downloaded from http://ajpcell.physiology.org/ by 10.220.33.1 on April 19, 2017

Statistical analyses. Differences between ^{86}Rb uptake groups were tested by one-way ANOVA, followed by multiple comparison using Student-Newman-Keuls, Bonferroni, and Tukey's post tests. $P < 0.001$ was considered to be very significant.

RESULTS

A yeast-2-hybrid screen of a mouse brain library of *Xho*I-(dT) primed clones inserted in pACT2 identified AATYK1 as a protein interacting with the regulatory, carboxyl-terminal end of SPAK (29). AATYK1 was also identified in a genome-wide screen as a protein containing two [S/V/G]RFx[V/I]xx[T/S/I/V]xx motifs (8). As we previously demonstrated that SPAK regulation of NKCC1 activity requires the presence of WNK4, a kinase acting upstream of SPAK (15), we first examined the possibility that AATYK1 also regulates NKCC1 activity. AATYK1 was cloned from mouse brain using RT-PCR, sequence verified and subcloned into the *Xenopus laevis* oocyte vector pBF. Oocytes were then injected with water or mouse NKCC1 cRNA in the presence or absence of AATYK1 cRNA. As indicated in Fig. 1, AATYK1 markedly inhibited the function of both endogenous frog as well as overexpressed mouse cotransporter. The levels of K^+ (^{86}Rb) uptakes were close to those measured in the presence of 20 μM bumetanide (Fig. 1). The nearly complete inhibition of NKCC1 activity observed by the presence of AATYK1 suggested the possibility that trafficking of the cotransporter to the plasma membrane might be impaired. We previously used an enhanced green fluorescent protein (EGFP)-tagged NKCC1 to confirm that SPAK/WNK4 did not alter cotransporter trafficking to the membrane (15). Confocal microscopy of *Xenopus laevis* oocytes co-expressing the same construct and AATYK1 revealed no difference in EGFP-NKCC1 expression in or near the plasma membrane (Fig. 2*A*). Although this method was validated using a membrane-specific fluorescent dye, FM 4–64 (24), this method is not definitive and might not exclude the possibility that the EGFP-NKCC1 signal originates from submembranous vesicles. In addition, the presence of the EGFP tag to the NH_2 terminus of NKCC1 did not alter the inhibitory effect of AATYK1 on cotransporter activity (Fig. 2*B* vs. Fig. 1).

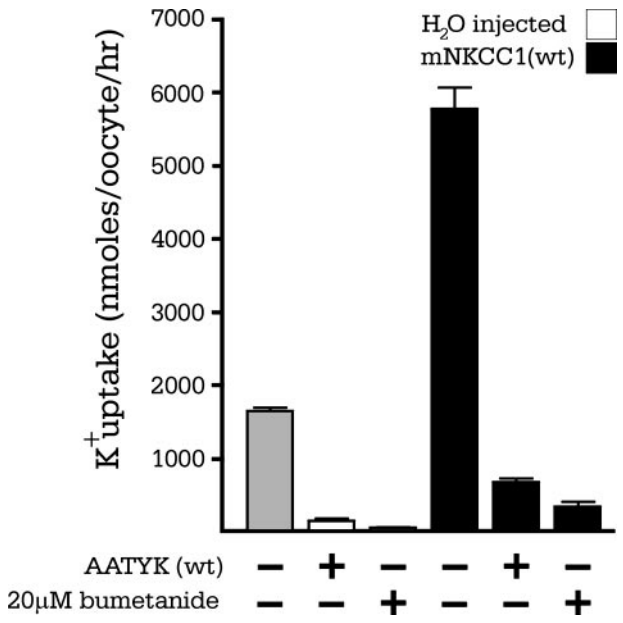

Fig. 1. Inhibition of frog and mouse Na-K-2Cl contransporter-1 (NKCC1) by apoptosis-associated tyrosine kinase (AATYK1). NKCC1 (15 ng) or water was injected into *Xenopus laevis* oocytes together with AATYK1 (10 ng). K^+ uptake was measured under isosmotic (195 mOsM) conditions. Incubation with 20 μM bumetanide confirmed that AATYK1 was affecting both endogenous and heterologously expressed NKCC1. Bars represent means ± SE (n = 20 oocytes). Each experimental condition was repeated twice with similar results.

To determine whether the catalytic activity of AATYK1 plays a role in the inhibition of NKCC1, we mutated conserved residues that are key to the catalytic activity of the kinase. The first mutant, K109E, targets a conserved lysine residue highly conserved in all protein kinases, which interacts with the β phosphate of ATP. When this conserved residue is mutated, AATYK1 was still capable of inhibiting cotransporter activity to the same extent than wild-type AATYK1 (Fig. 3). We also mutated two key aspartic acid residues: the first, D206A, targets the conserved catalytic aspartate in the catalytic loop (18), whereas the second, D224A, is responsible for chelating a magnesium ion that positions the phosphates for phosphotransfer (1, 27). Both additional catalytic mutants behaved similarly to the first mutant and wild-type AATYK1, inhibiting NKCC1 function (Fig. 3). In addition, co-expression of SPAK/WNK4 with each of the catalytically inactive AATYK1 mutants could only stimulate NKCC1 activity to levels similar to those observed with wild-type AATYK1 (Fig. 3).

Given that neither membrane trafficking nor the catalytic activity of AATYK1 appears responsible for the observed inhibition of NKCC1 function, we performed a yeast-two-hybrid analysis to identify possible accessory proteins which may be components of the regulatory cascade. Yeast two-hybrid analysis between AATYK1 and NKCC1 showed no protein-protein interaction between the cytosolic tails of the cotransporter and AATYK1 (Fig. 4, *A* and *B*). The presence of two SPAK binding motifs in the extreme COOH-terminus of AATYK1 suggests that inhibition of NKCC1 activity may involve the Ste20-related serine/threonine kinase. The regulatory domain of SPAK positively interacts with the regulatory domain of AATYK1 (Fig. 4*C*), confirming our previously reported data (29). However, when the phenylalanine residue within each SPAK binding motif was mutated into an alanine residue, no positive interaction was observed between SPAK and the mutant AATYK1 (Fig. 4*D*).

Regulation of NKCC1 activity has been linked to the state of phosphorylation of key threonine residues in the NH_2 terminus of the cotransporter (7, 14, 36). The use of specific pharmacological inhibitors, such as calyculin A, suggests a role for PP1 in the dephosphorylation and inhibition of cotransporter activity. In addition, studies by the Forbush group found NKCC1 co-immunoprecipitating with PP1 (6). However, our yeast two-hybrid analysis did not demonstrate protein-protein interaction between the NH_2 or COOH terminus of NKCC1 and PP1 (Fig. 4, *E* and *F*). We identified within AATYKI a putatively strong PP1 binding motif (KKKxVxFxD) within the regulatory COOH-terminus, upstream of the two SPAK binding motifs (5). Using yeast two-hybrid analysis, we demonstrated protein-protein interaction between full-length PP1 and the regulatory domain of AATYK1 (Fig. 4*G*). Because previous studies have demonstrated that mutation of the valine residue in the PP1 binding motif completely disrupts docking (25), we mutated V1175 of AATYK1 into an alanine residue.

Downloaded from http://ajpcell.physiology.org/ by 10.220.33.1 on April 19, 2017

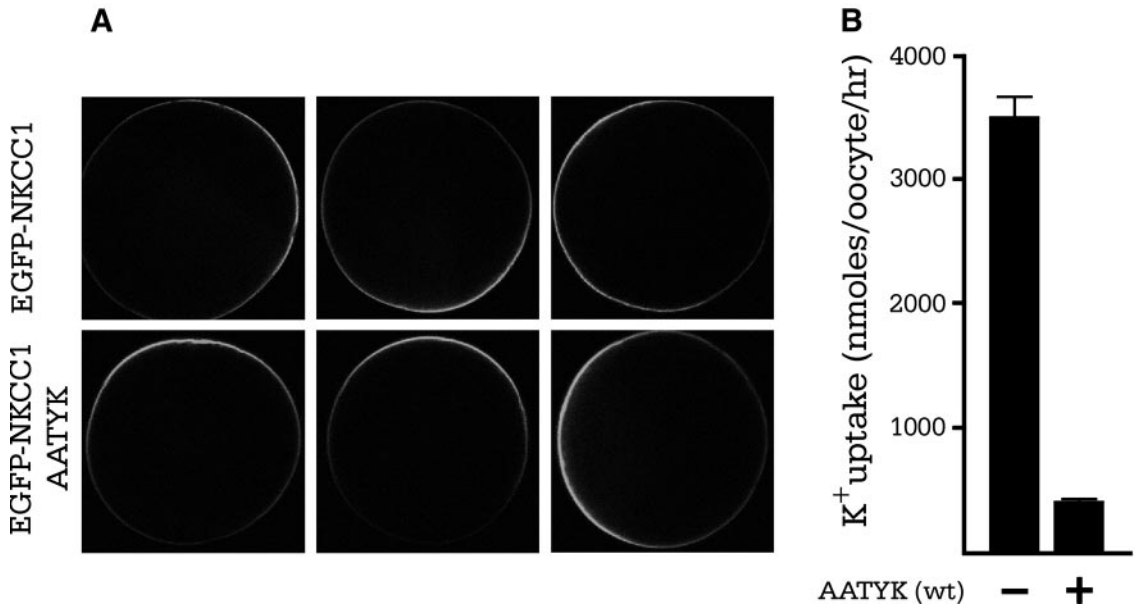

Fig. 2. Membrane expression of NKCC1 revealed by enhanced green fluorescent protein (EGFP) fluorescence is not affected by AATYK1. *A*: *Xenopus laevis* oocytes were injected with 15 ng of EGFP-NKCC1 cRNA and 10 ng of AATYK1 cRNA. Membrane fluorescence was observed 3 days postinjection using confocal laser microscopy. *Top*, three individual EGFP-NKCC1-injected oocytes; *bottom*, EGFP-NKCC1-injected oocytes expressing AATYK1. All images were captured using identical confocal microscopic settings (see MATERIALS AND METHODS). *B*: EGFP-NKCC1 (15 ng) was injected into *Xenopus laevis* oocytes together with AATYK1 (10 ng). K^+ uptake was measured in isosmotic (195 mOsM) conditions. Bars represent means ± SE (n = 20 oocytes). Confocal and flux experiments were repeated twice with identical results.

Here we demonstrate absence of interaction of this PP1-deficient AATYK1 mutant with PP1 (Fig. 4*H*). Despite the absence of a putative PP1 binding motif in either SPAK or WNK4, we also tested whether full-length PP1 interacted with either kinase. We observed no interaction between PP1 and SPAK or PP1 and WNK4 (data not shown).

To confirm the physical interaction observed among AATYK1, SPAK, and PP1, we performed co-immunoprecipitation studies using mammalian HEK-293 cells transfected with c-myc-tagged wild-type or mutant AATYK1s, together with HA-tagged PP1 and wild-type SPAK. Confirmation of protein expression is shown using immunoprecipitation of cell lysates with either a monoclonal anti-c-myc, polyclonal anti-SPAK, or monoclonal anti-HA antibodies, followed by Western blot analysis (Fig. 5*A*). Co-immunoprecipitations of cell lysates with anti-c-myc antibody followed by immunoblotting with either anti-HA antibody (Fig. 5*B*) or anti-SPAK antibody (Fig. 5*C*) confirm the protein-protein interactions identified through our yeast two-hybrid studies. We also took advantage of our AATYK1 mutants harboring the PP1 binding motif substitution V1175A, and the SPAK binding motif substitutions F1280A and F1290A. When the respective PP1 and SPAK binding motifs in AATYK1 are mutated, the proteins can no longer co-immunoprecipitate (Fig. 5*B*, *lane 2* and 5*C*, *lane 3*).

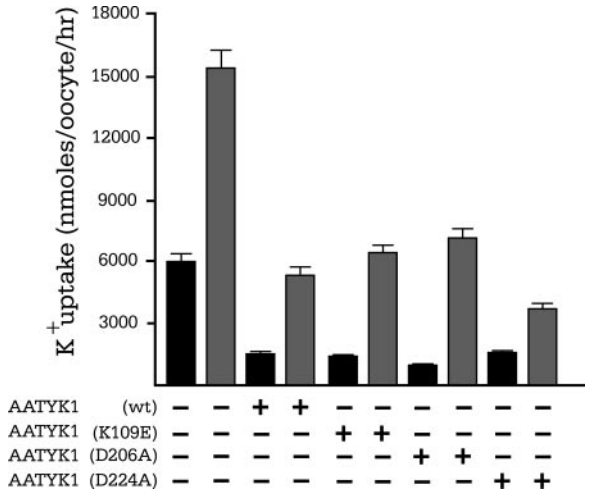

Fig. 3. AATYK1 catalytic activity is not required for NKCC1 inhibition. K^+ uptake in *Xenopus laevis* oocytes incubated in isosmotic (195 mOsM) conditions and expressing NKCC1 alone (black bars) or NKCC1, Ste-20-related proline kinase (SPAK), and with no kinase (WNK4; gray bars). Chart below bar graph depicts which form of AATYK was co-expressed: wild-type AATYK1 is denoted as (wt); catalytically inactive AATYK1 mutants are denoted as (K109E, D206A, and D224A), respectively. Bars represent means ± SE (n = 20 oocytes). Each experimental condition was repeated twice with similar results.

The absence of any yeast two-hybrid interaction between AATYK1 and the cotransporter, taken together with the positive interaction among AATYK1, SPAK, and PP1, suggests that AATYK1 exerts its effect on the cotransporter through either SPAK, PP1, or both. In the absence of SPAK-AATYK1 interaction, we observed no inhibition of NKCC1 function by AATYK1 (Fig. 6). In addition, when SPAK and WNK4 were co-expressed with the SPAK binding-deficient AATYK1 mutant and the cotransporter, we observed levels of NKCC1 activity similar to those observed with cotransporter alone (Fig. 6). These data indicate that the expression of SPAK alleviates the inhibitory effect of AATYK1 on cotransporter activity, and/or that the expression of AATYK1 reduces the activation of cotransporter function by SPAK and WNK4. When the PP1-deficient mutant form of AATYK1 (V1175A) was injected in *Xenopus laevis* oocytes, we also observed less co-

Downloaded from http://ajpcell.physiology.org/ by 10.220.33.1 on April 19, 2017

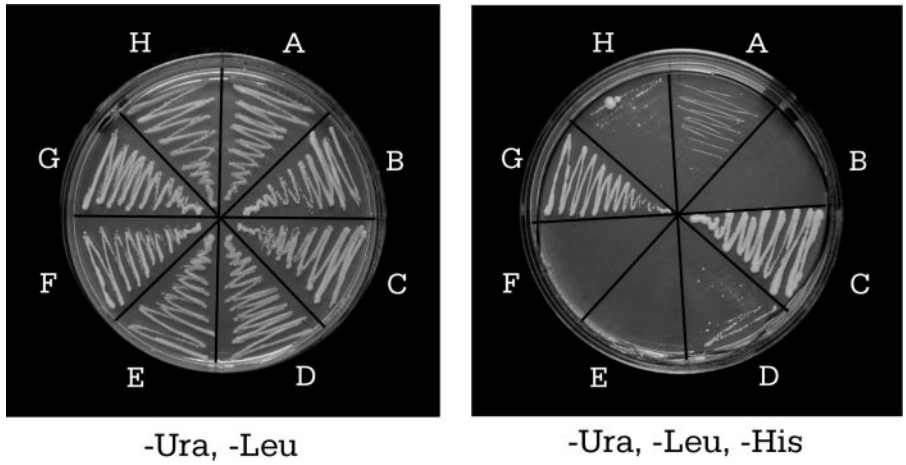

Fig. 4. Yeast 2-hybrid analysis showing the interactions among NKCC1, SPAK, protein phosphatase 1 (PP1), and AATYK1. Yeast transformed with different cDNA clones was plated onto agar plates lacking essential nutrients: uracil (Ura), leucine (Leu), and/or histidine (His). For each pair, the first clone was fused to the GAL4-activating domain in pACTII, and the second clone was fused to the GAL4-binding domain in pGBDUc2. A, AATYK1 + NKCC1_NT; *B*, AATYK1 + NKCC1_CT; C, SPAK + AATYK1; D, SPAK + AATYK1 (SPAK binding-deficient mutant); E, PP1 + NKCC1_NT; F, PP1 + NKCC1_CT; G, PP1 + AATYK1; H, PP1 + AATYK1 (PP1 binding-deficient mutant). *Left*, control plate lacking two essential nutrients (uracil and leucine) to demonstrate transformation efficiency. *Right*, yeast survival exists only upon interaction between the GAL4 fusion proteins translated from each clone. NKCC1_NT and NKCC1_CT are the NH_2 and COOH termini of the cotransporter, respectively. Each experimental condition was repeated twice with identical results.

transporter inhibition compared with wild-type AATYK1 (Fig. 6). In addition, coexpression of SPAK/WNK4 with the mutant AATYK1 resulted in a stimulation of NKCC1 activity similar to that observed in the absence of AATYK1 or with the SPAK binding-deficient form of AATYK1 (Fig. 6).

DISCUSSION

Cation-chloride cotransporters play major roles in ion absorption and secretion, cell volume regulation, cell survival and proliferation, neuronal excitability and control of blood pressure. NKCC1, in particular, is intimately involved with all these important biological processes, and as with most transport mechanisms, its regulation is rather complex. Elucidating the signaling transduction pathways involved in phosphorylation/dephosphorylation of the cotransporter is critical for understanding the regulation of the cotransporter and understanding its activation at the molecular level. Our laboratory and others have started identifying some of the molecules that interact and regulate the cotransporter (2, 10, 13, 15, 26, 29, 30, 35, 36). Among them are: SPAK and OSR1, the WNK kinases WNK1, WNK3, and WNK4, and now as a result of this study, AATYK1, a brain-enriched putative tyrosine kinase.

We previously demonstrated that the stimulatory effect of WNK4 on cotransporter function was due to a WNK4/SPAK

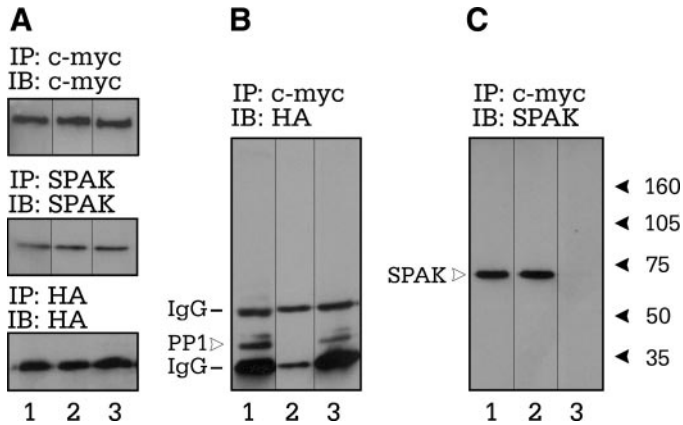

Fig. 5. Coimmunoprecipitation analysis confirming AATYK1-SPAK-PP1 interaction. Human embryonic kidney (HEK)-293 cells were transfected with hemagglutinin (HA)-tagged PP1, wild-type SPAK, and c-myc-tagged AATYK1 (wild-type: 1, V1175A: 2, and F1280A + F1290A: 3). Immunoprecipitations (IP) were performed with mouse anti-c-myc (*A–C*, *top*), rabbit anti-SPAK (*A*, *middle*), or mouse anti-HA antibodies (*A*, *bottom*). Note the presence of the heavy and light IgG chains when the mouse secondary antibody recognizes the immunoprecipitated mouse anti-c-myc antibody (*B*), in contrast to the absence of any IgG signal with the rabbit secondary antibody (*C*). IB, immunoblot.

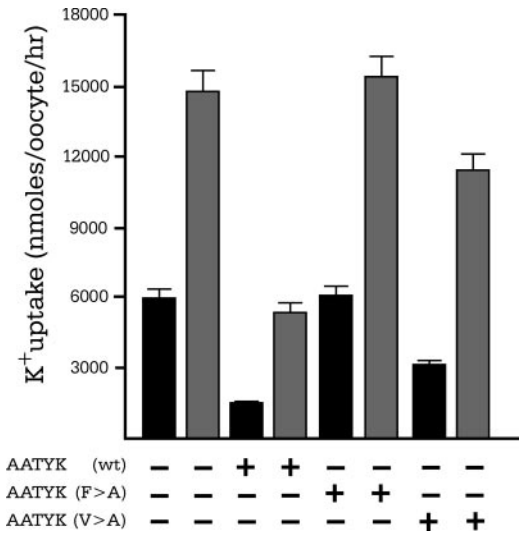

Fig. 6. SPAK and PP1 binding to AATYK1 are required for NKCC1 inhibition. K^+ uptake in *Xenopus laevis* oocytes incubated in isosmotic (195 mOsM) conditions and expressing NKCC1 alone (black bars) or NKCC1, SPAK, and WNK4 (gray bars). Chart below bar graph depicts which form of AATYK was co-expressed: Wild-type AATYK1 is denoted as (wt); SPAK-binding-deficient AATYK1 is denoted as (F>A); PP1-binding-deficient AATYK1 is denoted as (V>A). Bars represent means ± SE (n = 20 oocytes). Each experimental condition was repeated twice with similar results.

Downloaded from http://ajpcell.physiology.org/ by 10.220.33.1 on April 19, 2017

interaction, and not a result of WNK4/NKCC1 interaction (15). On the basis of the premise that AATYK1 is a putative protein kinase and that it interacts with SPAK (29), we examined its effect on NKCC1 function. Our data demonstrate that AATYK1 expression completely abolishes both *Xenopus* and murine NKCC1 function by affecting their activity, without apparent effect on trafficking within the resolution of the fluorescent assay. As both SPAK and WNK4 affect NKCC1 function through their catalytic activities (15), we examined whether AATYK1 also requires its kinase activity to modulate NKCC1 function. We independently mutated three residues highly conserved in kinases and critical for their catalytic function: a lysine residue that interacts with the β phosphate of ATP (K109), an aspartic acid residue conserved in the catalytic loop (D206) shown by Tomomura and coworkers (34) to prevent autophosphorylation of AATYK1, and another aspartate residue responsible for chelating magnesium (D224). In each case, the AATYK1 mutants inhibited NKCC1 function to an extent similar to wild-type AATYK1 alone or when SPAK and WNK4 are coexpressed. Thus, our results clearly indicate that the catalytic function of AATYK1 is not involved in cotransporter inhibition. Based on these results, the next logical hypothesis is that the AATYK1 effect was mediated through interactions with other proteins. We previously demonstrated that mutation of the conserved phenylalanine residue in the RFxV motif to an alanine prevents NKCC1-SPAK interaction in yeast and validated these yeast-two-hybrid data by an independent GST pull-down assay (29). Our yeast-two-hybrid analysis combined with co-immunoprecipitation studies clearly demonstrate that mutation of these key phenylalanine residues within the two RFxV motifs in AATYK1 prevent SPAK interaction. In contrast to the three catalytic mutants, the SPAK binding-deficient AATYK1 mutant was completely inert, unable to inhibit cotransporter function, indicating that AATYK1 affects NKCC1 function through its interaction with SPAK.

Perhaps our most surprising observation was the significant reduction in AATYK1 inhibition of NKCC1 when we mutated the conserved PP1 binding motif in the regulatory domain of the kinase. In other words, preventing PP1 binding to AATYK1 was almost as efficient as preventing SPAK interaction with AATYK1. The observation that the binding of both proteins appears to be necessary for the total AATYK1 effect on NKCC1 function, combined with the fact that the catalytic activity of AATYK1 is not required, indicates that the tyrosine kinase acts solely as a scaffold, bringing PP1 in close proximity to SPAK (Fig. 7*A*). This observation offers considerable insight into the regulation of NKCC1, placing the dephosphorylation of SPAK by PP1 as one of the critical limiting steps in the activation/deactivation of the cotransporter. The PP1-deficient AATYK1 mutant also demonstrates that overexpression of AATYK1 does not act as a "sink" for SPAK, simply pulling the Ste20 kinase away from the cotransporter. Whether the scaffolding role of AATYK1 is functionally relevant in tissues or reveals a mechanism of action that could involve other proteins with similar function is still unresolved. In fact, the NH_2-terminus of NKCC1 itself is a potential scaffold for both SPAK and PP1, as the kinase can bind to the first RFQV motif and the phosphatase can bind to the downstream RVNF motif. However, as the downstream RVNF site overlaps with a second SPAK binding site (6, 30), whether competition between the kinase and the phosphatase at the second site prevents PP1 dephosphorylation of SPAK and inactivation of the cotransporter is unknown. Interestingly, NKCC2, which shares sites of SPAK phosphorylation with NKCC1 and the first SPAK binding domain, lacks both the second SPAK binding and the overlapping PP1 binding motifs. To make the matter even more complex, we identified within the regulatory subunits of PP2A, strong motifs for SPAK interaction (8). Thus, as for AATYK1 and NKCC1, the regulatory subunit of PP2A likely scaffolds both SPAK as well as its catalytic subunit. In these three examples (Fig. 7*B*), the phosphatase is scaffolded in the vicinity of the kinase, indicating a critical role for scaffolding in mediating dephosphorylation of the kinase.

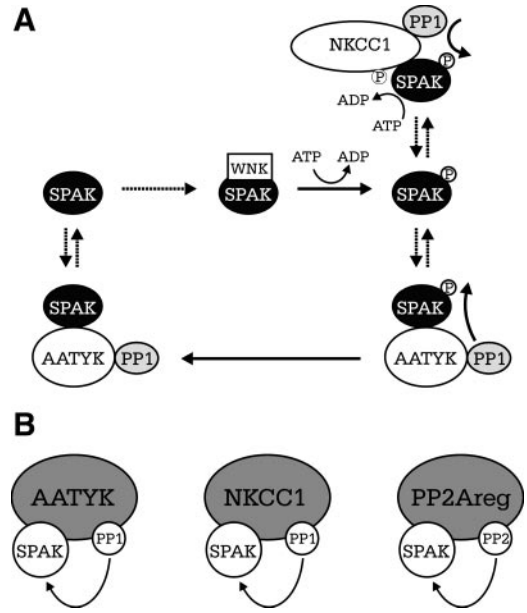

Fig. 7. Putative models representing macromolecular complex comprising NKCC1, SPAK, WNK4, AATYK1, and PP1. *A*: phosphorylation/dephosphorylation (solid arrows) pathways and binding (dashed arrows) interactions among PP1, SPAK, WNK4, AATYK1, and NKCC1 are depicted. *B*: AATYK1, NKCC1, and $PP2A_{REG}$ are each depicted as scaffolding subunits for SPAK and either PP1 or PP2A.

Using Northern blot analysis, Gaozza and coworkers (16) have shown expression of AATYK1 in kidney, heart, lung, skeletal muscle, and highest levels of expression in brain. These tissues also express NKCC1 in abundance (9). The fact that AATYK1 was shown to be upregulated during apoptosis (16) and neuronal differentiation (31) indicates an important role for the tyrosine kinase as a signaling molecule. In myeloid 32Dcl3 cells, AATYK1 mRNA is undetectable under control conditions. Upon exposure to cytokines, which induce terminal differentiation and apoptotic cell death, mRNA levels increase markedly to reach a plateau after 5–7 days. Since apoptosis is associated with a significant decrease in cell volume, and with a significant loss of K^+ and Na^+, ion transport pathways must be affected by programed cell death (11, 20, 21). Several studies in particular have shown that inhibition of NKCC1 by bumetanide does not trigger apoptosis (17) but rather protect cells against apoptotic cell death (12, 23, 28). In these studies, the activity of the Na-K-2Cl cotransporter increased intracellular Na^+, driving the Na^+/Ca^{2+} exchanger, which resulted in a net movement of Ca^{2+} ions into the cell leading to apoptosis.

Downloaded from http://ajpcell.physiology.org/ by 10.220.33.1 on April 19, 2017

By inhibiting the cotransporter and thus preventing Ca^{2+} entry, bumetanide protected against cell death. In contrast, during apoptosis, inhibition of NKCC1 function would prevent the movement of ions back into the cell and therefore facilitate the dehydration process. Whether AATYK1 is involved in shutting-off NKCC1 during apoptosis remains to be determined.

In conclusion, our findings suggest that AATYK1 indirectly inhibits cotransporter activity by scaffolding an inhibitory phosphatase (PP1) in proximity to a stimulatory kinase (SPAK), thus allowing PP1 to dephosphorylate SPAK. SPAK dephosphorylation, in turn, results in the inhibition of SPAK/WNK4 activation of the Na-K-2Cl cotransporter.

GRANTS

This work was supported by National Institutes of Health Grants NS-36758 and GM-074771 (E. Delpire) and an American Heart Association Fellowship Award (K. B. E. Gagnon).

REFERENCES

1. **Adams JA.** Kinetic and catalytic mechanisms of protein kinases. *Chem Rev* 101: 2271–2290, 2001.
2. **Anselmo AN, Earnest S, Chen W, Juang YC, Kim SC, Zhao Y, Cobb MH.** WNK1 and OSR1 regulate the Na^+, K^+, $2Cl^-$ cotransporter in HeLa cells. *Proc Natl Acad Sci USA* 103: 10883–10888, 2006.
3. **Baker SJ, Sumerson R, Reddy CD, Berrebi AS, Flynn DC, Reddy EP.** Characterization of an alternatively spliced AATYK mRNA: expression pattern of AATYK in the brain and neuronal cells. *Oncogene* 20: 1015–1021, 2001.
4. **Bar-Sagi D, Rotin D, Batzer A, Mandiyan V, Schlessinger J.** SH3 domains direct cellular localization of signaling molecules. *Cell* 74: 83–91, 1993.
5. **Cohen PTW.** Protein phosphatase 1-targeted in many directions. *J Cell Sci* 115: 241–256, 2002.
6. **Darman RB, Flemmer A, Forbush B.** Modulation of ion transport by direct targeting of protein phosphatase type 1 to the Na-K-Cl cotransporter. *J Biol Chem* 276: 34359–34362, 2001.
7. **Darman RB, Forbush B.** A regulatory locus of phosphorylation in the N terminus of the Na-K-Cl cotransporter, NKCC1. *J Biol Chem* 277: 37542–37550, 2002.
8. **Delpire E, Gagnon KB.** Genome-wide analysis of SPAK/OSR1 binding motifs. *Physiol Genomics* 28: 223–231, 2007.
9. **Delpire E, Rauchman MI, Beier DR, Hebert SC, Gullans SR.** Molecular cloning and chromosome localization of a putative basolateral Na-K-2Cl cotransporter from mouse inner medullary collecting duct (mIMCD-3) cells. *J Biol Chem* 269: 25677–25683, 1994.
10. **Dowd BF, Forbush B.** PASK (proline-alanine-rich STE20-related kinase), a regulatory kinase of the Na-K-Cl cotransporter (NKCC1). *J Biol Chem* 278: 27347–27353, 2003.
11. **Franco R, Bortner CD, Cidlowski JA.** Potential roles of electrogenic ion transport and plasma membrane depolarization in apoptosis. *J Membr Biol* 209: 43–58, 2006.
12. **Franco-Cea A, Valencia A, Sanchez-Armass S, Dominguez G, Moran J.** Role of ionic fluxes in the apoptotic cell death of cultured cerebellar granule neurons. *Neurochem Res* 29: 227–238, 2004.
13. **Gagnon KB, England R, Delpire E.** Characterization of SPAK and OSR1, regulatory kinases of the Na-K-2Cl cotransporter. *Mol Cell Biol* 26: 689–698, 2006.
14. **Gagnon KB, England R, Delpire E.** A single binding motif is required for SPAK activation of the Na-K-2Cl cotransporter. *Cell Physiol Biochem*. In Press.
15. **Gagnon KB, England R, Delpire E.** Volume sensitivity of cation-chloride cotransporters is modulated by the interaction of two kinases: SPAK and WNK4. *Am J Physiol Cell Physiol* 290: C134–C142, 2006.
16. **Gaozza E, Baker SJ, Vora RK, Reddy EP.** AATYK: a novel tyrosine kinase induced during growth arrest and apoptosis of myeloid cells. *Oncogene* 15: 3127–3135, 1997.
17. **Iwamoto LM, Fujiwara N, Nakamura KT, Wada RK.** Na-K-2Cl cotransporter inhibition impairs human lung cellular proliferation. *Am J Physiol Lung Cell Mol Physiol* 287: L510–L514, 2004.
18. **Johnson LN, Noble ME, Owen DJ.** Active and inactive protein kinases: structural basis for regulation. *Cell* 85: 149–158, 1996.
19. **Kawa S, Fujimoto J, Tezuka T, Nakazawa T, Yamamoto T.** Involvement of BREK, a serine/threonine kinase enriched in brain, in NGF signalling. *Genes Cells* 9: 219–232, 2004.
20. **Kim JA, Kang YY, Lee YS.** Activation of Na^+, K^+, Cl^--cotransport mediates intracellular Ca^{2+} increase and apoptosis induced by Pinacidil in HepG2 human hepatoblastoma cells. *Biochem Biophys Res Commun* 281: 511–519, 2001.
21. **Lang F, Foller M, Lang KS, Lang PA, Ritter M, Gulbins E, Vereninov A, Huber SM.** Ion channels in cell proliferation and apoptotic cell death. *J Membr Biol* 205: 147–157, 2005.
22. **Lytle C.** Activation of the avian erythrocyte Na-K-Cl cotransport protein by cell shrinkage, cAMP, fluoride, and calyculin-A involves phosphorylation at common sites. *J Biol Chem* 272: 15069–15077, 1997.
23. **Marklund L, Behnam-Motlagh P, Henriksson R, Grankvist K.** Bumetanide annihilation of amphotericin B-induced apoptosis and cytotoxicity is due to its effect on cellular K^+ flux. *J Antimicrob Chemother* 48: 781–786, 2001.
24. **Meade P, Hoover RS, Plata C, Vazquez N, Bobadilla NA, Gamba G, Hebert SC.** cAMP-dependent activation of the renal-specific Na^+-K^+-$2Cl^-$ cotransporter is mediated by regulation of cotransporter trafficking. *Am J Physiol Renal Physiol* 284: F1145–F1154, 2003.
25. **Meiselbach H, Sticht H, Enz R.** Structural analysis of the protein phosphatase 1 docking motif: molecular description of binding specificities identifies interacting proteins. *Chem Biol* 13: 49–59, 2006.
26. **Moriguchi T, Urushiyama S, Hisamoto N, Iemura SI, Uchida S, Natsume T, Matsumoto K, Shibuya H.** WNK1 regulates phosphorylation of cation-chloride-coupled cotransporters via the STE20-related kinases, SPAK and OSR1. *J Biol Chem* 580: 42685–42693, 2006.
27. **Nolen B, Taylor S, Ghosh G.** Regulation of protein kinases; controlling activity through activation segment conformation. *Mol Cell* 15: 661–675, 2004.
28. **O'Reilly N, Xia Z, Fiander H, Tauskela J, Small DL.** Disparity between ionic mediators of volume regulation and apoptosis in N1E 115 mouse neuroblastoma cells. *Brain Res* 943: 245–256, 2002.
29. **Piechotta K, Garbarini NJ, England R, Delpire E.** Characterization of the interaction of the stress kinase SPAK with the Na^+-K^+-$2Cl^-$ cotransporter in the nervous system: Evidence for a scaffolding role of the kinase. *J Biol Chem* 278: 52848–52856, 2003.
30. **Piechotta K, Lu J, Delpire E.** Cation chloride cotransporters interact with the stress-related kinases Ste20-related proline-alanine-rich kinase (SPAK) and oxidative stress response 1 (OSR1). *J Biol Chem* 277: 50812–50819, 2002.
31. **Raghunath M, Patti R, Bannerman P, Lee CM, Baker S, Sutton LN, Phillips PC, Damodar Reddy C.** A novel kinase, AATYK induces and promotes neuronal differentiation in a human neuroblastoma (SH-SY5Y) cell line. *Brain Res Mol Brain Res* 77: 151–162, 2000.
32. **Robinson DR, Wu Y, Lin S.** The protein tyrosine kinase family of the human genome. *Oncogene* 19: 5548–5557, 2000.
33. **Russell JM.** Sodium-potassium-chloride cotransport. *Physiol Rev* 80: 211–276, 2000.
34. **Tomomura M, Fernandez-Gonzales A, Yano R, Yuzaki M.** Characterization of the apoptosis-associated tyrosine kinase (AATYK) expressed in the CNS. *Oncogene* 20: 1022–1032, 2001.
35. **Vitari AC, Deak M, Morrice NA, Alessi DR.** The WNK1 and WNK4 protein kinases that are mutated in Gordon's hypertension syndrome, phosphorylate and active SPAK and OSR1 protein kinases. *Biochem J* 391: 17–24, 2005.
36. **Vitari AC, Thastrup J, Rafiqi FH, Deak M, Morrice NA, Karlsson HK, Alessi DR.** Functional interactions of the SPAK/OSR1 kinases with their upstream activator WNK1 and downstream substrate NKCC1. *Biochem J* 397: 223–231, 2006.
37. **Wang H, Brautigan DL.** A novel transmembrane Ser/Thr kinase complexes with protein phosphatase-1 and inhibitor-2. *J Biol Chem* 277: 49605–49612, 2002.

Downloaded from http://ajpcell.physiology.org/ by 10.220.33.1 on April 19, 2017